Contribution from the Department of Chemistry,
State University of New York at Buffalo, Buffalo, New York 14214

Dimeric (Pentamethylcyclopentadienyl)rhodium and -iridium Complexes. 5.[1-4] Structural Studies on the Homogeneous Hydrogenation Catalysts $[(\eta^5\text{-}C_5Me_5)IrBr]_2(\mu\text{-}Br)_2$ and $[(\eta^5\text{-}C_5Me_5)IrI]_2(\mu\text{-}I)_2$ and Systematics in the Series $[(\eta^5\text{-}C_5Me_5)IrX]_2(\mu\text{-}X)_2$ (X = Cl, Br, I)

MELVYN ROWEN CHURCHILL* and STUART ALAN JULIS

Received November 27, 1978

The complexes di-μ-bromo-dibromobis(η^5-pentamethylcyclopentadienyl)diiridium(III), $[(\eta^5\text{-}C_5Me_5)IrBr]_2(\mu\text{-}Br)_2$, and di-$\mu$-iodo-diiodobis($\eta^5$-pentamethylcyclopentadienyl)diiridium(III), $[(\eta^5\text{-}C_5Me_5)IrI]_2(\mu\text{-}I)_2$, have each been investigated by means of a single-crystal X-ray structural analysis. Crystal data are as follows. $[(\eta^5\text{-}C_5Me_5)IrBr]_2(\mu\text{-}Br)_2$: triclinic, space group $P\bar{1}$, a = 8.757 (1) Å, b = 8.956 (1) Å, c = 16.166 (2) Å, α = 91.51 (1)°, β = 104.95 (1)°, γ = 93.58 (1)°, V = 1221.4 (3) Å^3, Z = 2 (dimers). $[(\eta^5\text{-}C_5Me_5)IrI]_2(\mu\text{-}I)_2$: orthorhombic, space group $Pccn$, a = 13.410 (1) Å, b = 21.537 (3) Å, c = 9.084 (1) Å, V = 2623.6 (6) Å^3, Z = 4 (dimers). Diffraction data for each complex were collected with a Syntex $P2_1$ automated diffractometer (Mo Kα, 5° < 2θ < 45°) and the structures were solved by using the Syntex XTL structure determination system. Final discrepancy indices were R_F = 4.0% and R_{wF} = 3.9% for the bromo complex (3210 independent data) and R_F = 3.7% and R_{wF} = 2.9% for the iodo derivative (1724 reflections). The bromo complex crystallizes with two independent molecules in the unit cell, each having precise C_i symmetry. Dimensions of note are Ir···Ir = 3.911 (1) and 3.892 (1) Å, Ir–Br(terminal) = 2.515 (1) and 2.522 (1) Å, Ir–Br(bridging) = 2.574 (1) and 2.576 (1) Å in molecule I and 2.564 (1) and 2.567 (1) Å in molecule II, and Ir–Br–Ir = 98.80 (4) and 98.68 (4)°. The iodo complex also has precise C_i symmetry, the crystallographic asymmetric unit consisting of half of a dimeric molecule. Important dimensions are Ir···Ir = 4.072 (1) Å, Ir–I(terminal) = 2.694 (1) Å, Ir–I(bridging) = 2.707 (1) and 2.712 (1) Å, and Ir–I–Ir = 97.42 (2)°. The geometric details of these molecules and of the analogous chloro complex, $[(\eta^5\text{-}C_5Me_5)IrCl]_2(\mu\text{-}Cl)_2$, are compared and the structural trends outlined.

Introduction

A number of (pentamethylcyclopentadienyl)rhodium and -iridium complexes have been found to be useful catalysts in the homogeneous hydrogenation of olefins to alkanes and arenes to cyclohexanes and in a number of other reactions. The entire spectrum of these applications has recently been reviewed by Maitlis.[5] In general the catalytic activity of the dinuclear species shows the following tendencies.[5]

(1) Iridium complexes are usually 2–3 times as active as the analogous rhodium complexes but cause more isomerization of the substrate.

(2) The μ-hydride complexes are *less effective* hydrogenation catalysts roughly in proportion to the number of bridging hydride ligands present—e.g., the activity changes in the order $[(\eta^5\text{-}C_5Me_5)IrCl]_2(\mu\text{-}Cl)_2 > [(\eta^5\text{-}C_5Me_5)IrCl]_2(\mu\text{-}H)(\mu\text{-}Cl) > [(\eta^5\text{-}C_5Me_5)IrCl]_2(\mu\text{-}H)_2 > \{[(\eta^5\text{-}C_5Me_5)Ir]_2(\mu\text{-}H)_3\}^+$.

(3) The catalytic activity for a given variety of halide species varies in the order Cl > Br > I.

We have previously examined the crystal structures of a number of these species, including $[(\eta^5\text{-}C_5Me_5)RhCl]_2(\mu\text{-}H)(\mu\text{-}Cl)$,[1] $[(\eta^5\text{-}C_5Me_5)RhCl]_2(\mu\text{-}Cl)_2$,[2] $[(\eta^5\text{-}C_5Me_5)RhBr]_2(\mu\text{-}Br)_2$,[4] $[(\eta^5\text{-}C_5Me_5)Rh(Cl_{1-x}Br_x)]_2(\mu\text{-}(Cl_{1-x'}Br_{x'})_2)$,[4] $[(\eta^5\text{-}C_5Me_5)IrCl]_2(\mu\text{-}H)(\mu\text{-}Cl)$,[3] and $[(\eta^5\text{-}C_5Me_5)IrCl]_2(\mu\text{-}Cl)_2$.[3] We now report the results of X-ray structural analyses on the iridium bromide and iodide complexes $[(\eta^5\text{-}C_5Me_5)IrBr]_2(\mu\text{-}Br)_2$ and $[(\eta^5\text{-}C_5Me_5)IrI]_2(\mu\text{-}I)_2$, with a view toward examining the systematic changes in geometry as the halide ions change Cl → Br → I.

Experimental Section

The complexes were each prepared, as described previously,[6] by metathesis of $[(\eta^5\text{-}C_5Me_5)IrCl]_2(\mu\text{-}Cl)_2$ with the appropriate sodium halide in acetone. The products were each recrystallized from acetone.

Collection and Treatment of X-ray Diffraction Data. Data collection and all crystallographic computations were carried out by by using a Syntex $P2_1$ four-circle automated diffractometer and the Syntex XTL structure solution system.[7]

1. $[(\eta^5\text{-}C_5Me_5)IrBr]_2(\mu\text{-}Br)_2$. The crystal selected for the X-ray diffraction study was a rather large deep red parallelepiped with dimensions of 0.40 × 0.35 × 0.30 mm. It was mounted in air on a thin glass fiber and fixed into an aluminum pin in a eucentric goniometer. Measurement of unit cell parameters, determination of orientation matrix, surveys of 2θ and ω scans along the principal reciprocal cell axes, and data collection were carried out as described previously.[8] Data were corrected for absorption by an empirical method, based on a set of ψ scans.[9] Details appear in Table I.

2. $[(\eta^5\text{-}C_5Me_5)IrI]_2(\mu\text{-}I)_2$. A beautiful deep red parallelepiped of dimensions 0.30 × 0.25 × 0.20 mm was mounted, centered, and oriented as with the previous complex. Experimental details appear in Table I.

Solution and Refinement of the Structures. Analytical scattering factors[10a] for neutral Ir, I, Br, C, and H were used; contributions for all nonhydrogen atoms were corrected for both real and imaginary components of anomalous dispersion.[10b] The function minimized during the least-squares refinement process was $\sum w(|F_o| - |F_c|)^2$.

1. $[(\eta^5\text{-}C_5Me_5)IrBr]_2(\mu\text{-}Br)_2$. The structure was solved via a three-dimensional Patterson map. Refinement of positional and isotropic thermal parameters for the six independent heavy atoms led to R_F = 12.5% and R_{wF} = 15.3%. A difference-Fourier synthesis now led to the location of the 20 remaining nonhydrogen atoms. Continued full-matrix least-squares refinement, using anisotropic thermal parameters for all nonhydrogen atoms, led to convergence with R_F = 4.2%, R_{wF} = 4.3% and GOF = 2.29. A careful survey of $|F_o|$ vs. $|F_c|$ for low-angle reflections indicated the existence of secondary extinction. (The 101 reflection also appeared to show evidence of "clipping" by the lead backstop and was removed at this stage.) A secondary extinction correction was made to all data by using the approximation shown in eq 1; the resulting value for k was 2.052 × 10^{-7}. Continued

$$F_o^{cor} = F_o^{uncor}(1.0 + kI_{obsd}) \quad (1)$$

refinement led to final convergence with R_F = 4.0%, R_{wF} = 3.9%, and GOF = 2.12 for all 3210 reflections and R_F = 3.5% and R_{wF} = 3.9% for those 2921 reflections with $|F_o| > 3\sigma(F_o)$. A final difference-Fourier synthesis had three peaks of height 0.76, 0.71, and 0.67 e Å^{-3} as its most prominent features. There were no unambiguous indications of the positions of the hydrogen atoms. The residual, $\sum w(|F_o| - |F_c|)^2$, showed no significant variations as a function of $|F_o|$, $(\sin\theta)/\lambda$, Miller index, or serial number. The weighting scheme is thus acceptable. Final positional and thermal parameters appear in Table II.

2. $[(\eta^5\text{-}C_5Me_5)IrI]_2(\mu\text{-}I)_2$. The structure of this species was solved by the multiple tangent formula of Germain, Main, and Woolfson[11] by using the program MULTAN. Details appear in Table III (sup-

0020-1669/79/1318-1215$01.00/0

Table I. Details of Data Collection for $[(\eta^5\text{-}C_5Me_5)IrBr]_2(\mu\text{-}Br_2)$ and $[(\eta^5\text{-}C_5Me_5)IrI]_2(\mu\text{-}I)_2$

	$[IrBr]_2(\mu\text{-}Br)_2$ complex	$[IrI]_2(\mu\text{-}I)_2$ complex
	(A) Crystal Parameters	
crystal system	triclinic	orthorhombic
space group	$P\bar{1}$ [C_i^1; No. 2]	$Pccn$ [D_{2h}^{10}; No. 56]
a, Å	8.7571 (10)[a]	13.4103 (14)[b]
b, Å	8.9563 (12)	21.5373 (25)
c, Å	16.1655 (21)	9.0837 (14)
α, deg	91.507 (11)	
β, deg	104.951 (10)	
γ, deg	93.584 (10)	
V, Å^3	1221.4 (3)	2623.6 (6)
Z	2 (dimers)	4 (dimers)
mol wt	974.52	1162.52
ρ(obsd), g cm^{-3}	2.70 (2)[c]	
ρ(calcd), g cm^{-3}	2.65	2.94
temp, °C	24	24
	(B) Collection of Intensity Data	
diffractometer	Syntex $P2_1$	
radiation	Mo Kα ($\bar{\lambda}$ 0.710 730 Å)	
monochromator	highly oriented graphite; equatorial geometry	
reflections measd	$\pm h, \pm k, +l$ (one form)	$+h, \pm k, +l$ (two forms)
2θ range, deg	5.0–45.0	
scan type	coupled θ (crystal)–2θ (counter)	
scan speed	2.0°/min in 2θ	
scan range	$[2\theta(K\alpha_1) - 0.9]°$–$[2\theta(K\alpha_2) + 0.9]°$	
bdg measurement	at beginning and end of 2θ scan; each for one-fourth of total scan time	
standards	3 every 97 reflections; no significant decay	3 every 97 reflections; 2% linear decay (corrected)
reflections collected	3346 total, yielding 3211 independent	3448 total, yielding 1725 independent
data averaging	$R(I)$ = 1.4% for 135 pairs of averaged reflections	$R(I)$ = 2.3% for 1723 pairs of averaged reflections
absorption coeff	184.8 cm^{-1}	155.1 cm^{-1}
reflections used for empirical absorption correction: hkl, 2θ, T_{max}/T_{min}[d,e]	$21\bar{3}$, 11.79°, 2.01 $31\bar{4}$, 16.33°, 1.93 $42\bar{8}$, 26.46°, 1.83 6,2,$\bar{10}$, 35.51°, 1.59 7,2,$\bar{13}$, 43.31°, 1.55	212, 10.99°, 1.64 204, 18.98°, 1.62 325, 24.62°, 1.56 636, 33.38°, 1.58

[a] Based on 24 reflections with 2θ = 23–30°. [b] Based on 24 reflections with 2θ = 20–28°. [c] Not on the data crystal. [d] See ref 9. [e] Each absorption curve was composed of the average of two curves (hkl and $\overline{hkl}$).

Table II. Final Positional and Anisotropic Thermal Parameters[a] for $[(C_5Me_5)IrBr]_2(\mu\text{-}Br)_2$

atom	x	y	z	B_{11}	B_{22}	B_{33}	B_{12}	B_{13}	B_{23}
Ir(1)	0.10400 (5)	0.04763 (5)	−0.09050 (3)	2.013 (20)	1.858 (20)	2.021 (20)	0.312 (14)	0.790 (15)	0.058 (14)
Ir(2)	0.60269 (5)	0.45268 (5)	0.41015 (3)	2.127 (21)	2.150 (21)	1.971 (20)	−0.123 (15)	0.699 (15)	−0.414 (15)
Br(1B)	−0.17720 (12)	−0.00343 (13)	−0.07139 (7)	1.97 (5)	3.35 (5)	2.29 (5)	0.13 (4)	0.51 (4)	0.26 (4)
Br(1T)	0.11353 (16)	−0.22819 (13)	−0.12039 (8)	4.61 (7)	2.20 (5)	4.36 (6)	0.51 (5)	1.87 (5)	−0.41 (4)
Br(2B)	0.34245 (13)	0.55077 (15)	0.42609 (7)	2.48 (5)	4.72 (6)	2.15 (5)	0.97 (4)	0.32 (4)	−0.56 (4)
Br(2T)	0.71925 (18)	0.71953 (15)	0.42252 (10)	5.81 (8)	2.72 (6)	5.89 (8)	−1.33 (5)	3.13 (6)	−0.99 (5)
C(11)	0.3040 (13)	0.1986 (12)	−0.0924 (7)	2.7 (5)	2.3 (5)	3.2 (5)	−0.2 (4)	1.6 (4)	0.3 (4)
C(12)	0.2522 (14)	0.1133 (12)	−0.1729 (7)	3.2 (6)	2.5 (5)	3.0 (5)	0.2 (4)	1.7 (5)	0.5 (4)
C(13)	0.0903 (15)	0.1431 (13)	−0.2108 (7)	4.3 (7)	3.1 (6)	1.5 (5)	−0.9 (5)	0.6 (4)	1.0 (4)
C(14)	0.0480 (14)	0.2520 (13)	−0.1566 (8)	3.4 (6)	3.1 (6)	3.8 (6)	1.1 (5)	1.9 (5)	2.2 (5)
C(15)	0.1749 (15)	0.2825 (11)	−0.0826 (7)	4.8 (7)	0.6 (4)	3.1 (5)	0.1 (4)	1.4 (5)	0.6 (4)
C(16)	0.4681 (15)	0.2059 (15)	−0.0320 (9)	3.0 (6)	4.3 (7)	4.8 (7)	−0.0 (5)	−0.0 (5)	0.7 (6)
C(17)	0.3523 (17)	0.0166 (15)	−0.2122 (9)	6.1 (8)	3.5 (6)	5.6 (8)	0.2 (6)	4.6 (7)	−0.6 (6)
C(18)	−0.0077 (18)	0.0828 (21)	−0.2977 (8)	5.7 (9)	10.5 (12)	1.1 (5)	−2.1 (8)	−0.6 (5)	0.7 (6)
C(19)	−0.1111 (17)	0.3241 (18)	−0.1763 (11)	3.9 (7)	6.2 (9)	8.7 (10)	2.8 (6)	2.6 (7)	3.6 (8)
C(110)	0.1844 (18)	0.3925 (13)	−0.0077 (8)	6.9 (8)	1.9 (5)	4.3 (7)	0.4 (5)	2.7 (6)	−0.4 (5)
C(21)	0.7634 (14)	0.3559 (14)	0.3488 (8)	2.8 (6)	3.5 (6)	3.4 (6)	−0.3 (5)	1.1 (5)	−1.9 (5)
C(22)	0.6278 (16)	0.4003 (13)	0.2845 (7)	4.9 (7)	2.5 (5)	2.6 (5)	−0.2 (5)	1.4 (5)	−0.7 (4)
C(23)	0.4937 (15)	0.3151 (13)	0.2962 (8)	4.5 (7)	2.2 (5)	3.5 (6)	0.6 (5)	1.4 (5)	−1.2 (5)
C(24)	0.5438 (14)	0.2211 (12)	0.3674 (7)	3.4 (6)	1.9 (5)	3.0 (5)	−0.0 (4)	1.3 (4)	−0.9 (4)
C(25)	0.7098 (14)	0.2452 (12)	0.3989 (7)	3.8 (6)	2.2 (5)	2.8 (5)	1.0 (4)	0.8 (5)	−0.7 (4)
C(26)	0.9381 (16)	0.4114 (18)	0.3572 (10)	2.8 (6)	6.8 (9)	7.2 (9)	−0.9 (6)	2.6 (6)	−2.5 (7)
C(27)	0.6324 (21)	0.5077 (17)	0.2147 (9)	9.9 (12)	4.8 (8)	3.8 (7)	0.7 (8)	4.0 (7)	1.4 (6)
C(28)	0.3267 (17)	0.3237 (18)	0.2436 (9)	3.7 (7)	7.5 (10)	4.1 (7)	1.7 (6)	−1.1 (5)	−2.4 (7)
C(29)	0.4346 (21)	0.1069 (17)	0.3964 (10)	7.9 (10)	3.9 (7)	6.8 (9)	−2.3 (7)	3.7 (8)	−0.6 (7)
C(210)	0.8105 (18)	0.1638 (17)	0.4716 (9)	5.9 (8)	5.3 (8)	3.5 (6)	2.2 (7)	−1.0 (6)	−0.2 (6)

[a] The anisotropic thermal parameters enter the equation for the calculated structure factor in the form $\exp[-{}^1/_4(h^2a^{*2}B_{11} + \ldots + 2hka^*b^*B_{12} + \ldots)]$.

Table IV. Final Positional and Anisotropic Thermal Parameters[a] for $[(C_5Me_5)IrI]_2(\mu\text{-}I)_2$

atom	x	y	z	B_{11}	B_{22}	B_{33}	B_{12}	B_{13}	B_{23}
Ir	0.00329 (2)	0.40780 (1)	0.04930 (4)	2.473 (17)	1.859 (16)	2.885 (17)	−0.021 (12)	0.019 (13)	0.167 (13)
I(B)	0.13123 (4)	0.49865 (3)	−0.03468 (7)	2.41 (3)	2.49 (3)	5.22 (3)	0.163 (20)	0.59 (2)	0.72 (3)
I(T)	−0.03538 (6)	0.37812 (3)	−0.23315 (7)	7.98 (4)	3.59 (3)	3.38 (3)	−0.08 (3)	−0.71 (3)	−0.68 (3)
C(1)	−0.0514 (6)	0.3751 (4)	0.2613 (10)	3.1 (4)	4.0 (5)	3.2 (4)	−0.1 (4)	0.5 (4)	1.1 (4)
C(2)	0.0469 (7)	0.3943 (4)	0.2782 (9)	4.3 (4)	3.0 (4)	2.1 (4)	0.5 (4)	−0.0 (3)	0.4 (3)
C(3)	0.1099 (6)	0.3568 (4)	0.1846 (10)	3.7 (4)	2.9 (4)	3.7 (4)	0.3 (4)	−0.2 (4)	1.1 (4)
C(4)	0.0459 (8)	0.3138 (4)	0.1094 (11)	5.5 (5)	2.1 (4)	4.4 (5)	0.9 (4)	−0.1 (5)	1.6 (4)
C(5)	−0.0546 (7)	0.3262 (4)	0.1551 (11)	3.4 (4)	2.8 (4)	4.5 (5)	−1.3 (4)	−0.5 (4)	1.6 (4)
C(6)	−0.1398 (8)	0.3980 (7)	0.3483 (12)	4.1 (5)	9.0 (9)	4.3 (6)	0.9 (6)	1.7 (4)	−0.2 (6)
C(7)	0.0846 (10)	0.4454 (6)	0.3786 (12)	6.1 (6)	5.9 (6)	3.5 (5)	−0.2 (5)	−0.7 (5)	0.3 (5)
C(8)	0.2218 (7)	0.3597 (5)	0.1735 (15)	3.1 (5)	5.2 (6)	6.2 (7)	0.6 (4)	0.4 (5)	1.5 (5)
C(9)	0.0819 (11)	0.2628 (5)	0.0086 (17)	8.1 (8)	2.1 (6)	8.5 (9)	1.1 (5)	0.2 (7)	−0.2 (5)
C(10)	−0.1453 (10)	0.2899 (6)	0.1096 (17)	5.5 (6)	4.7 (7)	8.3 (9)	−1.7 (5)	−2.3 (7)	2.1 (6)

atom	x	y	z	B, Å^2 [b]	atom	x	y	z	B, Å^2
H(6A)	−0.130 (8)	0.441 (6)	0.382 (14)	8.0	H(8C)	0.246 (10)	0.389 (5)	0.201 (15)	8.0
H(6B)	−0.211 (8)	0.391 (5)	0.291 (13)	8.0	H(9A)	0.072 (8)	0.215 (5)	0.091 (12)	8.0
H(6C)	−0.162 (8)	0.389 (6)	0.497 (12)	8.0	H(9B)	0.153 (8)	0.260 (7)	−0.014 (13)	8.0
H(7A)	0.101 (9)	0.427 (6)	0.487 (14)	8.0	H(9C)	0.042 (9)	0.245 (7)	−0.051 (14)	8.0
H(7B)	0.017 (9)	0.440 (6)	0.448 (13)	8.0	H(10A)	−0.141 (9)	0.271 (6)	0.022 (13)	8.0
H(7C)	0.154 (8)	0.452 (6)	0.361 (13)	8.0	H(10B)	−0.207 (8)	0.315 (5)	0.155 (12)	8.0
H(8A)	0.251 (10)	0.360 (5)	0.064 (12)	8.0	H(10C)	−0.139 (8)	0.260 (6)	0.169 (13)	8.0
H(8B)	0.247 (8)	0.318 (5)	0.228 (12)	8.0					

[a] See footnote *a* to Table II. [b] The isotropic thermal parameter was set at this value and not refined.

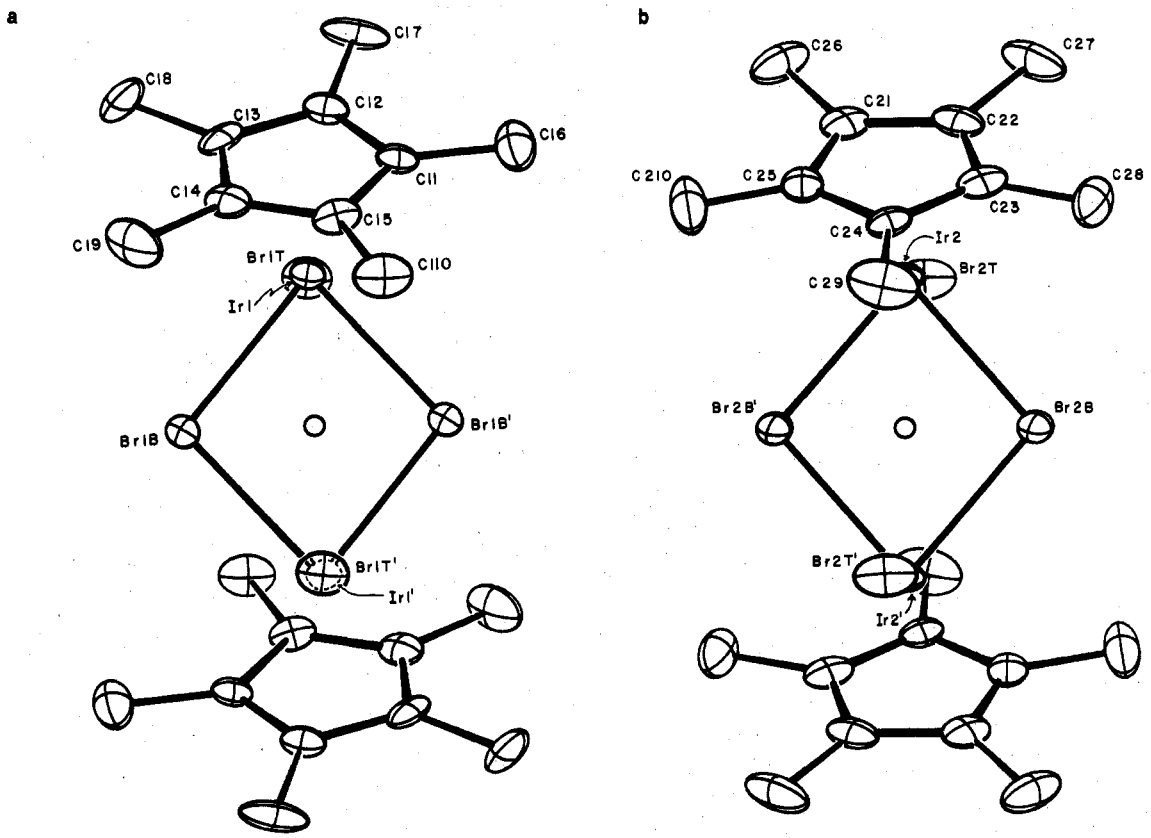

Figure 1. Labeling of atoms in the $[(\eta^5\text{-}C_5Me_5)IrBr]_2(\mu\text{-}Br)_2$ molecules: (a) molecule I, projected onto its $Ir(\mu\text{-}Br)_2Ir$ plane; (b) molecule II, rotated by 5° (about the vertical axis) from its $Ir(\mu\text{-}Br)_2Ir$ plane (ORTEP-II diagrams).

plementary material). The resulting "*E*-map", from the best solution, contained three independent peaks close to a crystallographic center of symmetry. The $Ir_2I_2(\mu\text{-}I)_2$ core was thus located. Refinement of positional and isotropic thermal parameters for the three independent "heavy" atoms led to convergence with $R_F = 13.7\%$ and $R_{wF} = 17.0\%$. A difference-Fourier map now resulted in the location of the 10 independent carbon atoms. Further refinement, using anisotropic thermal parameters, led to convergence with $R_F = 3.9\%$, $R_{wF} = 3.2\%$, and GOF = 1.33. A secondary extinction correction was again necessary, a value of $k = 1.07 \times 10^{-6}$ being calculated. A second difference-Fourier map suggested the positions of all hydrogen atoms. Continued refinement of all positional parameters and anisotropic thermal parameters for nonhydrogen atoms (with each hydrogen atom assigned an isotropic thermal parameter of 8.0 Å^2) led to final convergence with $R_F = 3.7\%$, $R_{wF} = 2.9\%$, and GOF = 1.21 for all 1724 independent reflections and with $R_F = 2.9\%$ and $R_{wF} = 2.8\%$ for those 1481 reflections with $|F_o| > 3\sigma(F_o)$. A final difference-Fourier synthesis was "clean" (ρ(max) = 0.84 e Å^{-3}) and the usual tests (vide infra) showed the weighting scheme to be appropriate. Final positional and thermal parameters are collected in Table IV.

Results and Discussion

The complex $[(\eta^5\text{-}C_5Me_5)IrBr]_2(\mu\text{-}Br)_2$ crystallizes in the centrosymmetric triclinic space group $P\bar{1}$ with two unrelated

Table V. Selected Intramolecular Distances (with Esd's) for $[(\eta\text{-}C_5Me_5)IrBr]_2(\mu\text{-}Br)_2$ and $[(\eta^5\text{-}C_5Me_5)IrI]_2(\mu\text{-}I)_2$

$[IrBr]_2(\mu\text{-}Br)_2$ molecule I		$[IrBr]_2(\mu\text{-}Br)_2$ molecule II		$[IrI]_2(\mu\text{-}I)_2$	
atoms	dist, A	atoms	dist, A	atoms	dist, A
		(A) Distances within the Ir_2X_4 Core			
Ir(1)···Ir(1′)	3.911 (1)	Ir(2)···Ir(2′)	3.892 (1)	Ir···Ir′	4.072 (1)
Ir(1)-Br(1B)	2.574 (1)	Ir(2)-Br(2B)	2.564 (1)	Ir-I(B)	2.712 (1)
Ir(1)-Br(1B′)	2.576 (1)	Ir(2)-Br(2B′)	2.567 (1)	Ir-I(B′)	2.707 (1)
Ir(1)-Br(1T)	2.515 (1)	Ir(2)-Br(2T)	2.522 (1)	Ir-I(T)	2.694 (1)
		(B) Iridium-Carbon Distances			
Ir(1)-C(11)	2.152 (12)	Ir(2)-C(21)	2.131 (12)	Ir-C(1)	2.178 (9)
Ir(1)-C(12)	2.154 (12)	Ir(2)-C(22)	2.142 (12)	Ir-C(2)	2.179 (8)
Ir(1)-C(13)	2.123 (11)	Ir(2)-C(23)	2.156 (12)	Ir-C(3)	2.182 (9)
Ir(1)-C(14)	2.163 (12)	Ir(2)-C(24)	2.157 (11)	Ir-C(4)	2.174 (9)
Ir(1)-C(15)	2.147 (10)	Ir(2)-C(25)	2.158 (12)	Ir-C(5)	2.149 (9)
av	2.148	av	2.149	av	2.172
		(C) Iridium-C(Methyl) Contacts			
Ir(1)···C(16)	3.299 (13)	Ir(2)···C(26)	3.303 (15)	Ir···C(6)	3.331 (11)
Ir(1)···C(17)	3.306 (15)	Ir(2)···C(27)	3.283 (15)	Ir···C(7)	3.286 (11)
Ir(1)···C(18)	3.268 (12)	Ir(2)···C(28)	3.248 (14)	Ir···C(8)	3.306 (10)
Ir(1)···C(19)	3.320 (16)	Ir(2)···C(29)	3.322 (16)	Ir···C(9)	3.316 (11)
Ir(1)···C(110)	3.294 (12)	Ir(2)···C(210)	3.284 (15)	Ir···C(10)	3.274 (13)
av	3.297	av	3.288	av	3.303
		(D) Distances within the $\eta^5\text{-}C_5Me_5$ Ring			
C(11)-C(12)	1.442 (16)	C(21)-C(22)	1.447 (18)	C(1)-C(2)	1.389 (13)
C(12)-C(13)	1.437 (18)	C(22)-C(23)	1.417 (19)	C(2)-C(3)	1.445 (12)
C(13)-C(14)	1.423 (17)	C(23)-C(24)	1.436 (16)	C(3)-C(4)	1.436 (13)
C(14)-C(15)	1.413 (17)	C(24)-C(25)	1.412 (18)	C(4)-C(5)	1.435 (13)
C(15)-C(11)	1.435 (17)	C(25)-C(21)	1.428 (17)	C(5)-C(1)	1.429 (13)
av	1.430	av	1.428	av	1.423
		(E) Carbon-Methyl Distances			
C(11)-C(16)	1.512 (18)	C(21)-C(26)	1.549 (19)	C(1)-C(6)	1.508 (15)
C(12)-C(17)	1.509 (19)	C(22)-C(27)	1.508 (19)	C(2)-C(7)	1.517 (14)
C(13)-C(18)	1.511 (17)	C(23)-C(28)	1.498 (20)	C(3)-C(8)	1.505 (13)
C(14)-C(19)	1.534 (20)	C(24)-C(29)	1.521 (20)	C(4)-C(9)	1.508 (16)
C(15)-C(110)	1.524 (17)	C(25)-C(210)	1.511 (18)	C(5)-C(10)	1.504 (16)
av	1.518	av	1.517	av	1.508

Table VI. Selected Interatomic Angles (with Esd's) for $[(\eta^5\text{-}C_5Me_5)IrBr]_2(\mu\text{-}Br)_2$ and $[(\eta^5\text{-}C_5Me_5)IrI]_2(\mu\text{-}I)_2$

$[IrBr]_2(\mu\text{-}Br)_2$ molecule I		$[IrBr]_2(\mu\text{-}Br)_2$ molecule II		$[IrI]_2(\mu\text{-}I)_2$	
atoms	angle, deg	atoms	angle, deg	atoms	angle, deg
		(A) Angles within the $Ir(\mu\text{-}X)_2Ir$ Bridges			
Ir(1)-Br(1B)-Ir(1′)	98.80 (4)	Ir(2)-Br(2B)-Ir(2′)	98.68 (4)	Ir-I(B)-Ir′	97.42 (2)
Br(1B)-Ir(1)-Br(1B′)	81.20 (4)	Br(2B)-Ir(2)-Br(2B′)	81.32 (4)	I(B)-Ir-I(B′)	82.58 (2)
Ir(1′)···Ir(1)-Br(1B)	40.62 (3)	Ir(2′)···Ir(2)-Br(2B)	40.69 (3)	Ir′···Ir-I(B)	41.25 (1)
Ir(1′)···Ir(1)-Br(1B′)	40.58 (3)	Ir(2′)···Ir(2)-Br(2B′)	40.63 (3)	Ir′···Ir-I(B′)	41.33 (1)
		(B) Angles Involving the Terminal Halogen Ligands			
Br(1B)-Ir(1)-Br(1T)	89.14 (4)	Br(2B)-Ir(2)-Br(2T)	88.77 (5)	I(B)-Ir-I(T)	91.44 (2)
Br(1B′)-Ir(1)-Br(1T)	89.50 (4)	Br(2B′)-Ir(2)-Br(2T)	90.11 (5)	I(B′)-Ir-I(T)	90.09 (2)
		(C) Internal Angles of the $\eta^5\text{-}C_5Me_5$ Ligand			
C(15)-C(11)-C(12)	107.8 (10)	C(25)-C(21)-C(22)	108.5 (10)	C(5)-C(1)-C(2)	108.8 (8)
C(11)-C(12)-C(13)	107.6 (10)	C(21)-C(22)-C(23)	106.6 (11)	C(1)-C(2)-C(3)	108.9 (8)
C(12)-C(13)-C(14)	107.5 (10)	C(22)-C(23)-C(24)	108.9 (11)	C(2)-C(3)-C(4)	106.9 (8)
C(13)-C(14)-C(15)	109.3 (11)	C(23)-C(24)-C(25)	108.0 (10)	C(3)-C(4)-C(5)	107.7 (8)
C(14)-C(15)-C(11)	107.7 (10)	C(24)-C(25)-C(21)	108.0 (10)	C(4)-C(5)-C(1)	107.7 (8)
		(D) External Angles of the $\eta^5\text{-}C_5Me_5$ Ligand			
C(12)-C(11)-C(16)	126.1 (10)	C(22)-C(21)-C(26)	125.4 (11)	C(2)-C(1)-C(6)	126.2 (9)
C(15)-C(11)-C(16)	126.1 (10)	C(25)-C(21)-C(26)	126.0 (11)	C(5)-C(1)-C(6)	124.9 (9)
C(11)-C(12)-C(17)	126.2 (11)	C(21)-C(22)-C(27)	126.0 (12)	C(1)-C(2)-C(7)	126.8 (8)
C(13)-C(12)-C(17)	126.2 (11)	C(23)-C(22)-C(27)	127.3 (12)	C(3)-C(2)-C(7)	124.3 (8)
C(12)-C(13)-C(18)	125.3 (11)	C(22)-C(23)-C(28)	125.4 (12)	C(2)-C(3)-C(8)	126.8 (8)
C(14)-C(13)-C(18)	126.9 (11)	C(24)-C(23)-C(28)	125.7 (12)	C(4)-C(3)-C(8)	126.2 (9)
C(13)-C(14)-C(19)	124.8 (12)	C(23)-C(24)-C(29)	124.3 (11)	C(3)-C(4)-C(9)	124.5 (9)
C(15)-C(14)-C(19)	125.9 (12)	C(25)-C(24)-C(29)	127.5 (11)	C(5)-C(4)-C(9)	127.7 (9)
C(11)-C(15)-C(110)	124.1 (10)	C(21)-C(25)-C(210)	127.0 (11)	C(1)-C(5)-C(10)	126.3 (9)
C(14)-C(15)-C(110)	128.0 (11)	C(24)-C(25)-C(210)	125.0 (11)	C(4)-C(5)-C(10)	125.7 (9)

dimeric molecules (each having crystallographically required C_i symmetry) in the unit cell. The molecules are separated by normal van der Waals distances; there are no abnormally short intermolecular distances. Molecule I (see Figure 1a) is centered on the inversion center at (0, 0, 0), while molecule II (see Figure 1b) is centered on the inversion center at ($^1/_2$,

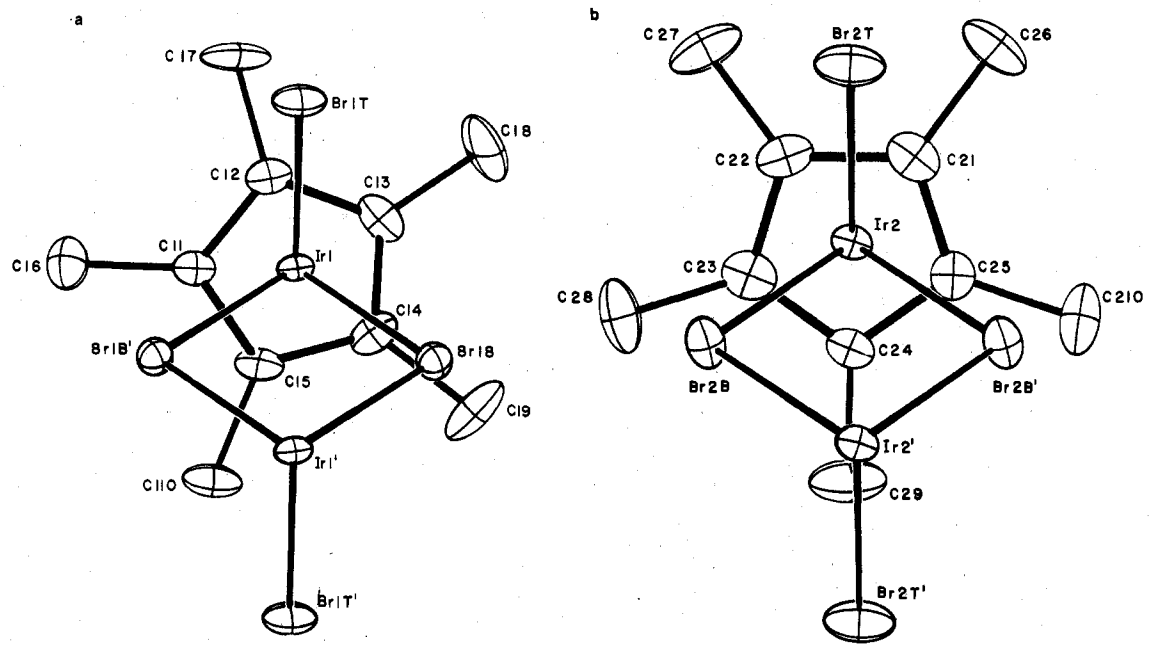

Figure 2. The $[(\eta^5\text{-}C_5Me_5)IrBr]_2(\mu\text{-}Br)_2$ molecules, projected onto their carbocyclic rings: (a) molecule I; (b) molecule II—note the approximate mirror plane.

$^1/_2$, $^1/_2$). The two crystallographically independent molecules have closely similar bond lengths (Table V) and bond angles (Table VI), but the detailed coordination geometry about the iridium atoms and overall molecular geometry vary substantially. Each iridium(III) ion is linked to an η^5-pentamethylcyclopentadienyl ligand and three bromide ligands (one terminal and two bridging). The relative orientations of η^5-C_5Me_5 ligands and $IrBr_3$ groups are different in the two molecules—in molecule I the terminal bromide ligand Br(1T) lies such that the Ir(1)–Br(1T) bond passes over the C(12)–C(13) bond of the carbocyclic ring (see Figure 2a); Br(1T) is, however, much closer to C(12) than to C(13). In molecule II, the Ir(2)–Br(2T) bond passes symmetrically over the C(21)–C(22) bond of the cyclopentadienyl system (see Figure 2b). This results in the η^5-$C_5Me_5IrBr_3$ moiety (and this entire $[(\eta^5\text{-}C_5Me_5)IrBr]_2(\mu\text{-}Br)_2$ molecule) having an approximate mirror plane passing through Br(2T), Ir(2), C(24), C(29), Ir(2′), Br(2T′), C(24′), and C(29′). Molecule II therefore has approximate C_{2h} symmetry, whereas molecule I has only C_i symmetry. The observation of varying rotomeric conformations of the η^5-C_5Me_5 system about the Ir···ring axis is not surprising in view of the facts that (i) complexes of either η^5-C_5Me_5 or η^5-C_5H_5 ligands show but a single resonance in their ^{1}H NMR spectra (in the absence of heteronuclear coupling) and (ii) that the barrier to rotation of the η^5-C_5H_5 rings in ferrocene, $(\eta^5\text{-}C_5H_5)_2Fe$, has been estimated as only 0.9 ± 0.3 kcal/mol.[12]

The $[(\eta^5\text{-}C_5Me_5)IrI]_2(\mu\text{-}I)_2$ molecule crystallizes in the centrosymmetric orthorhombic space group *Pccn*, the basic molecule (as defined by the positional parameters in Table IV) lying on the inversion center at (0, $^1/_2$, 0). As with the nonisomorphous bromo complex, there are no abnormally short intermolecular contacts. The overall molecular geometry is illustrated in Figure 3, while the relative orientations of the η^5-C_5Me_5 ligand and the IrI_3 fragment are shown in Figure 4. Bond lengths and angles are collected, with those for the bromo complex, in Tables V and VI. Important least-squares planes for the two species are compiled in Table VII.

Important intramolecular distances for the three species $[(\eta^5\text{-}C_5Me_5)IrX]_2(\mu\text{-}X)_2$ (X = Cl,[3] Br, I) are collected in Table VIII. The following systematic effects occur as the halide is changed, sequentially, from chloride, to bromide, and to iodide.

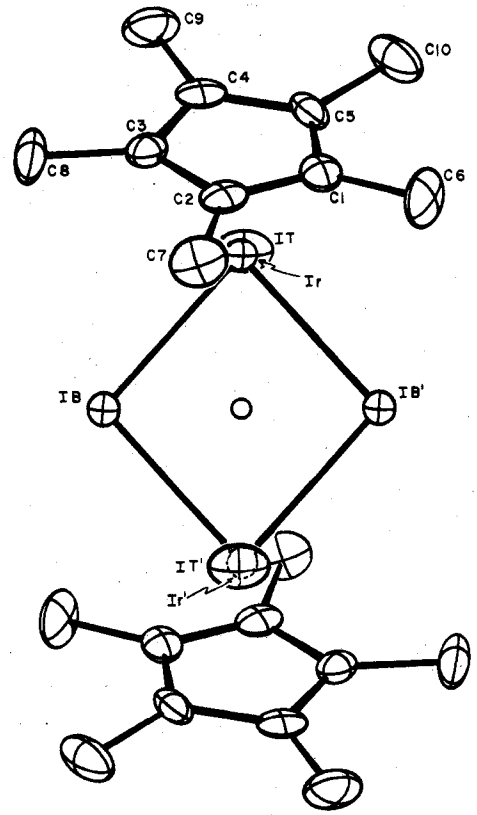

Figure 3. The $[(\eta^5\text{-}C_5Me_5)IrI]_2(\mu\text{-}I)_2$ molecule, projected onto its $Ir(\mu\text{-}I)_2Ir$ plane.

(1) The (nonbonding) iridium···iridium distance increases from 3.769 (1) Å in the chloride to 3.902 [13] Å[13] in the bromide and 4.072 (1) Å in the iodide. That these are clearly nonbonding interactions is indicated by (a) the "electron-precise" (cf. ref 14) nature of the complex, with each Ir(III) atom obeying the 18-electron (EAN) rule, and (b) the pronounced lengthening of the Ir···Ir separation relative to $[(\eta^5\text{-}C_5Me_5)IrCl]_2(\mu\text{-}H)(\mu\text{-}Cl)$,[3] where the two-electron, three-center $Ir(\mu\text{-}H)Ir$ linkage results in an Ir---Ir distance of 2.903 (1) Å. The average Ir–Ir bond length in the iridium(0) cluster, $Ir_4(CO)_{12}$, is 2.693 Å.[15]

Table VII

Least-Squares Planes and Atomic Deviations Therefrom (with Esd's) for $[(\eta^5\text{-}C_5Me_5)IrBr]_2(\mu\text{-}Br)_2$ and $[(\eta^5\text{-}C_5Me_5)IrI]_2(\mu\text{-}I)_2$ (Å)[a]

(A) $[(\eta^5\text{-}C_5Me_5)IrBr]_2(\mu\text{-}Br)_2$ Molecules

I: $Ir(\mu\text{-}Br)_2Ir$ Plane–Molecule I

$0.1579X - 0.9683Y - 0.1935Z = 0.0000$

Ir(1)[b]	0.000	Br (1B)[b]	0.000
Ir(1′)[b]	0.000	Br (1B′)[b]	0.000
Br(1T)	2.5150 (12)		

II: C(11)–C(15) Plane–Molecule I

$0.4248X + 0.7732Y - 0.4709Z = 3.3482$

C(11)[b]	−0.000 (11)	C(16)	0.077 (14)
C(12)[b]	0.014 (11)	C(17)	0.121 (14)
C(13)[b]	−0.023 (12)	C(18)	0.049 (18)
C(14)[b]	0.023 (12)	C(19)	0.103 (17)
C(15)[b]	−0.014 (11)	C(110)	0.032 (13)
Ir(1)	−1.7700 (4)		

III: $Ir(\mu\text{-}Br)_2Ir$ Plane–Molecule II

$0.3455X + 0.9350Y + 0.0796Z = 5.1744$

Ir(2)[b]	0.000	Br(2B)[b]	0.000
Ir(2′)[b]	0.000	Br(2B′)[b]	0.000
Br(2T)	−2.5210 (14)		

IV: C(21)–C(25) Plane–Molecule II

$-0.3480X + 0.6946Y + 0.6296Z = 3.7183$

C(21)[b]	−0.001 (12)	C(26)	0.086 (16)
C(22)[b]	−0.003 (12)	C(27)	0.076 (15)
C(23)[b]	0.006 (12)	C(28)	0.011 (15)
C(24)[b]	−0.007 (11)	C(29)	0.079 (16)
C(25)[b]	0.005 (11)	C(210)	0.047 (15)
Ir(2)	−1.7724 (4)		

(B) $[(\eta^5\text{-}C_5Me_5)IrI]_2(\mu\text{-}I)_2$ Molecule

V: $Ir(\mu\text{-}I)_2Ir$ Plane

$0.1754X + 0.2203Y + 0.9595Z = 2.3724$

Ir[b]	0.000	I(B)[b]	0.000
Ir′[b]	0.000	I(B′)[b]	0.000
I(T)	2.6936 (6)		

VI: C(1)–C(5) Plane

$-0.1119X + 0.6628Y - 0.7404Z = 3.6835$

C(1)[b]	−0.009 (9)	C(6)	−0.134 (13)
C(2)[b]	0.004 (8)	C(7)	0.001 (12)
C(3)[b]	0.003 (9)	C(8)	−0.049 (13)
C(4)[b]	−0.009 (9)	C(9)	−0.113 (13)
C(5)[b]	0.011 (9)	C(10)	−0.064 (14)
Ir	1.8013 (3)		

Dihedral Angles

plane I/plane II	126.2°	plane V/plane VI	125.7°
plane III/plane IV	125.4°		

[a] The equations of planes are expressed in Cartesian (Å) coordinates. [b] These atoms were used in calculating the plane.

(2) The terminal iridium–halide distances increase from 2.387 (4) Å in the chloride to 2.519 [5] Å in the bromide and 2.694 (1) Å in the iodide. The successive increments of 0.132 and 0.175 Å may be compared to changes in the covalent radius of the halogen atoms[16] by 0.15 and 0.19 Å, respectively.

(3) The bridging iridium–halide distances increase from 2.453 [5] Å in the chloride to 2.570 [6] Å in the bromide and 2.710 [4] Å in the iodide. The increments of 0.117 and 0.140 Å are slightly, but significantly, *smaller* than for the terminal iridium–halide linkages.

(4) The difference between terminal and bridging iridium–halide linkages decreases markedly with increasing size of halide. Individual differences are 0.066 Å for the chloride, 0.051 Å for the bromide, and 0.016 Å for the iodide. We attribute this trend to the easier polarizability and decreased electronegativity of the larger covalently linked halide ligands.

(5) The halogen···halogen separation within the $Ir(\mu\text{-}X)_2Ir$ bridge increases from 3.141 (6) Å in the chloride to 3.348 [6] Å in the bromide and 3.576 (1) Å in the iodide. These contacts are, in each case, significantly shorter than those predicted from van der Waals radii[17] (viz., Cl···Cl = 3.6 Å, Br···Br = 3.9 Å, and I···I = 4.3 Å).

(6) The angles at the bridging halides are, in each case, greater than 90°—thereby providing another diagnostic for the lack of any iridium···iridium bonding interaction. There is, however, a slight decrease in the Ir–X(B)–Ir′ angle as a function of size of halogen—e.g., 100.45 (12)° for the chloride, 98.74 [8]° for the bromide, and 97.42 (2)° for the iodide. In

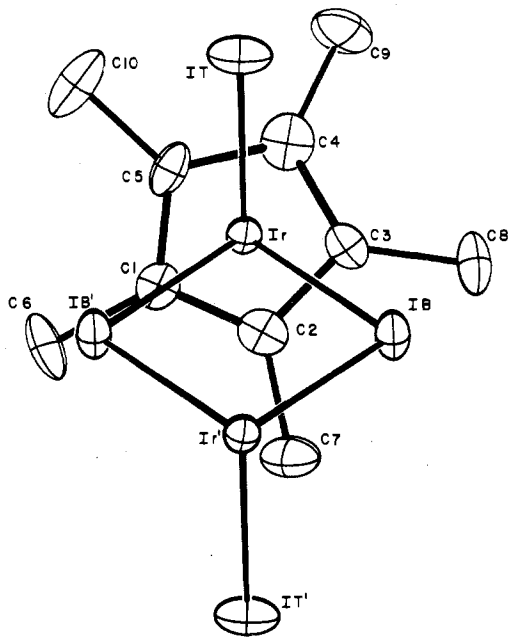

Figure 4. The $[(\eta^5\text{-}C_5Me_5)IrI]_2(\mu\text{-}I)_2$ molecule, projected onto its carbocyclic ring.

Table VIII. Average Intramolecular Distances (Å) and Angles (deg) with Esd's[a] for the Species $[(\eta\text{-}C_5Me_5)IrX]_2(\mu\text{-}X)_2$ (X = Cl, Br, I)

atoms	$[IrCl]_2(\mu\text{-}Cl)_2$[b]	$[IrBr]_2(\mu\text{-}Br)_2$	$[IrI]_2(\mu\text{-}I)_2$
Ir···Ir	3.769 (1)	3.902 [13]	4.072 (1)
Ir–X(T)	2.387 (4)	2.519 [5]	2.694 (1)
Ir–X(B)	2.453 [5]	2.570 [6]	2.710 [4]
X...X	3.141 (6)	3.348 [6]	3.576 (1)
Ir–X(B)–Ir′	100.45 (12)	98.74 [8]	97.42 (2)
X(B)–Ir–X(B′)	79.55 (12)	81.26 [8]	82.58 (2)
X(B)–Ir–X(T)	89.07 [82]	89.38 [57]	90.77 [95]
Ir–C (ring)	2.132 [16]	2.148 [13]	2.172 [13]
Ir–Cp[c]	1.7563 (4)	1.7712 [17]	1.8013 (3)
Ir···C(Me)	3.280 [33]	3.293 [23]	3.303 [23]
r(X)[d]	0.99	1.14	1.33

[a] Esd's on individual distances or angles are enclosed in parentheses. Esd's on average distances, enclosed in square brackets, are calculated using the "scatter formula" $[\sigma] = [\Sigma(d_i - \bar{d})^2/(N-1)]^{1/2}$. Here d_i is the ith of N equivalent distances and $\bar{d}$ is the average distance. Note that this result provides the "scatter" of values about the average value—i.e., it is an external estimate of the esd on an individual value. The precision of determination of the average value is given by $[\Sigma(d_i - \bar{d})^2/N(N-1)]^{1/2}$. [b] See ref 3. [c] Ir–Cp is the perpendicular distance from the iridium atom to the pentaatomic carbocyclic ring (see Table VII). [d] These are the covalent radii, taken from: Pauling, L. "The Nature of the Chemical Bond", 3rd ed.; Cornell University Press: Ithaca, N.Y., 1960; p 224.

sharp contrast to this, we note that the Ir–Cl(B)–Ir angle in the species $[(\eta^5\text{-}C_5Me_5)IrCl]_2(\mu\text{-}H)(\mu\text{-}Cl)$ is reduced to 72.65 (8)° as a result of the associated Ir–H(B)–Ir bonding system.[3]

(7) The X(B)–Ir–X(B′) angles, which are precisely supplementary to the Ir–X(B)–Ir′ angles (due to precise C_i symmetry of each molecule), show a slight increase with increasing size of halogen—i.e., 79.55 (12)° for the chloride, 81.26 [8]° for the bromide, and 82.58 (2)° for the iodide.

(8) An unexpected, but nevertheless unambiguous, result is that the bonding of the η^5-C_5Me_5 ligand to the iridium(III) center is strongest for the chloride, intermediate for the bromide, and weakest for the iodide. There are three distinct measurements indicating this. (a) The average Ir–C(ring) distance increases from 2.132 [16] Å in the chloride to 2.148 [13] Å in the bromide and 2.172 [13] Å in the iodide. (b) The perpendicular distance from the iridium(III) ion to the pentaatomic carbocyclic ring increases from 1.7563 (4) Å in the chloride to 1.7712 [17] Å in the bromide and 1.8013 (3) Å in the iodide. (c) The iridium···methyl interactions (Ir···C(Me)) from 3.280 [33] Å in the chloride to 3.292 [23] Å in the bromide and 3.303 [23] Å in the iodide. The stronger η^5-C_5Me_5→Ir bonding for the chloride is believed to be a result of the (highly electronegative) chloride ligands removing charge from the iridium atom.

Acknowledgment. This work was supported by the National Science Foundation through Grant No. CHE77-04981 (to M.R.C.).

Registry No. $[(\eta^5\text{-}C_5Me_5)IrBr]_2(\mu\text{-}Br)_2$, 55971-89-6; $[(\eta^5\text{-}C_5Me_5)IrI]_2(\mu\text{-}I)_2$, 33040-12-9.

Supplementary Material Available: A table of data-processing formulas, Table III, and two listings of structure factor amplitudes (27 pages). Ordering information is given on any current masthead page.

References and Notes

(1) Part 1: Churchill, M. R.; Ni, S. W.-Y. *J. Am. Chem. Soc.* **1973**, *95*, 2150.
(2) Part 2: Churchill, M. R.; Julis, S. A.; Rotella, F. J. *Inorg. Chem.* **1977**, *16*, 1137.
(3) Part 3: Churchill, M. R.; Julis, S. A. *Inorg. Chem.* **1977**, *16*, 1488.
(4) Part 4: Churchill, M. R.; Julis, S. A. *Inorg. Chem.* **1978**, *17*, 3011.
(5) Maitlis, P. M. *Acc. Chem. Res.* **1978**, *11*, 301.
(6) Gill, D. S.; Maitlis, P. M. *J. Organomet. Chem.* **1975**, *87*, 359.
(7) The Syntex XTL system has been described previously: Churchill, M. R.; Lashewycz, R. A. *Inorg. Chem.* **1978**, *17*, 1950.
(8) Churchill, M. R.; Lashewycz, R. A.; Rotella, F. J. *Inorg. Chem.* **1977**, *16*, 265.
(9) Using the program TAPER: Churchill, M. R.; Hollander, F. J. *Inorg. Chem.* **1978**, *17*, 1950 (see Experimental Section, p 1951, column 1).
(10) "International Tables for X-Ray Crystallography"; Kynoch Press: Birmingham, England, 1974; Vol. IV: (a) pp 99–101; (b) pp 149–150.
(11) Germain, G.; Main, P.; Woolfson, M. M. *Acta Crystallogr., Sect. A* **1971**, *27*, 368.
(12) Bohn, R. K.; Haaland, A. *J. Organomet. Chem.* **1966**, *5*, 470.
(13) Esd's on averaged distances, etc., are shown in square brackets—see footnote *a* to Table VIII.
(14) Mason, R.; Mingos, D. M. P. *J. Organomet. Chem.* **1973**, *50*, 53.
(15) Churchill, M. R.; Hutchinson, J. P. *Inorg. Chem.* **1978**, *17*, 3528.
(16) See footnote *d* to Table VIII.
(17) Pauling, L. "The Nature of the Chemical Bond", 3rd ed.; Cornell University Press: Ithaca, N.Y., 1960; p 260.

Contribution from the Materials and Molecular Research Division, Lawrence Berkeley Laboratory, and the Department of Chemistry, University of California, Berkeley, California 94720

Chloro-, Methyl-, and (Tetrahydroborato)tris((hexamethyldisilyl)amido)thorium(IV) and -uranium(IV). Crystal Structure of (Tetrahydroborato)tris((hexamethyldisilyl)amido)thorium(IV)

HOWARD W. TURNER, RICHARD A. ANDERSEN,* ALLAN ZALKIN,* and DAVID H. TEMPLETON*

Received December 4, 1978

Reaction of sodium (hexamethyldisilyl)amide with thorium tetrachloride or uranium tetrachloride yields chlorotris((hexamethyldisilyl)amido)thorium(IV) or -uranium(IV), respectively. The chloroamides of thorium or uranium react with dimethylmagnesium or methyllithium yielding the methyl derivatives $MeTh[N(SiMe_3)_2]_3$ or $MeU[N(SiMe_3)_2]_3$, respectively. The chloro compounds yield $BH_4M[N(SiMe_3)_2]_3$ upon reaction with lithium tetrahydroborate, where M is thorium or uranium. Infrared spectra of the tetrahydroborate derivatives suggest that BH_4^- is bonded in a tridentate fashion in both compounds, the metal atoms being six-coordinate. Single-crystal X-ray analysis of the thorium borohydride confirms the infrared result. The white $BH_4Th[N(Si(CH_3))_2]_3$ crystals are rhombohedral with cell dimensions a_r = 11.137 Å and α_r = 113.61°; the triply primitive hexagonal cell has a_h = 18.640 (3) Å, c_h = 8.604 (1) Å, V = 2489 Å^3, Z = 3, and D_x = 1.40 g/cm^3, space group $R3m$. The structure was refined by full-matrix least squares to a conventional R factor of 0.031 for 1014 data. The Th atom is on a threefold axis 2.32 Å from three nitrogen atoms and 2.61 Å from the boron atom, a distance which represents a triple bridge bond between Th and B. The three (dimethylsilyl)amide ligands are disordered by a mirror plane parallel to the threefold axis. $CH_3Th[N(Si(CH_3)_3)_2]_3$ is isomorphous with $BH_4Th[N(Si(CH_3)_3)_2]_3$ with cell dimensions a_h = 18.68 (1) Å and c_h = 8.537 (6) Å. The diffraction data yielded f'' = 12.16 ± 0.33 e for the imaginary scattering term for Th with Cu Kα radiation.

Introduction

Tris((hexamethyldisilyl)amido)metal compounds have been described for a large group of p-, d-, and 4f-block metal atoms.[1-3] In contrast, only four silylamido compounds have been described for the 5f-block series, $ClTh[N(SiMe_3)_2]_3$,[4] $O_2U[N(SiMe_3)_2]_2(THF)_2$, $OU[N(SiMe_3)_2]_3$, and $U[N(SiMe_3)_2]_3$.[5] This paper describes the series $XM[N(SiMe_3)_2]_3$, where M is thorium or uranium and X is chloro, methyl, or tetrahydroborate. The crystal structure of one of these compounds, $(BH_4)Th[N(SiMe_3)_2]_3$, is also described.

* To whom correspondence should be addressed: R.A.A., Department of Chemistry; A.Z. and D.H.T., Lawrence Berkeley Laboratory.

Results and Discussion

Sodium (hexamethyldisilyl)amide reacts with thorium or uranium tetrachloride affording chlorotris((hexamethyldisilyl)amido)thorium or -uranium, respectively. The air- and moisture-sensitive, monomeric (by mass spectrometry) amides are readily soluble in pentane from which they may be crystallized. Physical properties of the compounds are shown in Table I.

0020-1669/79/1318-1221$01.00/0